Heterobimetallic Complexes of Rhenium and Ruthenium Containing Methylaminobis(difluorophosphine)

Joel T. Mague* and Zhaiwei Lin

Department of Chemistry, Tulane University, New Orleans, Louisiana 70118

Received March 22, 1994®

The syntheses of cpRuCl(η^1-MeN(PF_2)$_2$)$_2$ (**1**) and *fac*-ReBr(CO)$_3$(η^1-MeN(PF_2)$_2$)$_2$ (**3**) are described together with their use in the directed synthesis of heterobimetallic complexes. The monodentate MeN(PF_2)$_2$ ligands in **1** are cleaved on exposure to moisture or on chromatography on Florisil to give cpRu(P(O)F_2)(PF_2NHMe)$_2$ (**2**). With $Co_2(CO)_8$ **1** and **3** respectively yield cpRu(μ-MeN(PF_2)$_2$)$_2$Co(CO)$_2$ (**4**) and *fac*-Re(CO)$_3$(μ-MeN(PF_2)$_2$)$_2$Co(CO)$_2$ (**5**), while with IrCl(CO)(PPh_3)$_2$, cpRu(μ-MeN(PF_2)$_2$)$_2$IrCl$_2$(PPh_3) (**6**) and *fac*-Re(CO)$_3$(μ-MeN(PF_2)$_2$)$_2$IrClBr(PPh_3) (**7**) are obtained. Complex **1** and [RhCl(CO)$_2$]$_2$ yield cpRu(μ-MeN(PF_2)$_2$)$_2$RhCl$_2$ (**8**) which adds dimethylphenylphosphine to give cpRu(μ-MeN(PF_2)$_2$)$_2$RhCl$_2$(PMe_2Ph) (**9**) while with **3** the product is *fac*-Re(CO)$_3$(μ-MeN(PF_2)$_2$)$_2$RhClBr (**10**). A complex mixture of products is formed from **1** and Pt(L)(PPh_3)$_2$ (L = C_2H_4, C_2Ph_2) which has not been completely characterized, but *fac*-Re(CO)$_3$(μ-MeN(PF_2)$_2$)$_2$PtBr(PPh_3) (**11**), in which the platinum adopts a distorted square pyramidal coordination with a very long apical Pt–Br bond, is obtained from **3** and Pt(C_2Ph_2)(PPh_3)$_2$. The structures of **2**, **5**, **9**, and **11** have been determined by X-ray crystallography. **2**: monoclinic; $P2_1/n$; a = 10.487(2), b = 11.832(2), c = 11.910(2) Å; β = 90.50(1)°; Z = 4. **5**: triclinic; $P\bar{1}$; a = 9.794(1), b = 10.563(1), c = 9.624(2) Å; α = 98.06(1), β = 101.29(1), γ = 81.796(9)°; Z = 2. **9**: monoclinic; $P2_1/c$; a = 18.239(3), b = 8.195(2), c = 18.078(2) Å, β = 102.36(1)°; Z = 4. **11**: monoclinic; $C2/m$; a = 12.649(2), b = 14.908(1), c = 19.798(2) Å; β = 96.600(9)°; Z = 4.

Introduction

Much interest has been shown in recent years in the chemistry of heterobimetallic complexes.[1–3] Of particular concern is the development of directed routes to specific complexes, particularly those in which the metals are connected by "robust" ligands so that fragmentation of the complexes in their subsequent reactions is inhibited. One particularly successful route involves the use of "metalloligands" in which ligands already bound to one metal have free coordination sites that can bind a second metal.[2–10] We have previously reported on the use of *mer*-M(CO)$_3$(η^2-MeN(P(OPr^i)$_2$)$_2$)(η^1-MeN(P(OPr^i)$_2$)$_2$) (M = Mo, W) to form heterobimetallic complexes with rhodium and iridium[8] and on the similar chemistry of *fac*-Mo(CO)$_3$(η^2-MeN(PF_2)$_2$)(η^1-MeN(PF_2)$_2$) and cpFeCl(η^1-MeN(PF_2)$_2$)$_2$[9,10] and describe here further work in this area.

Experimental Section

Materials and Measurements. All reactions were carried out under an atmosphere of prepurified nitrogen using standard Schlenk techniques. Solvents were purified by standard methods and were distilled under nitrogen just prior to use. Literature methods were used to prepare MeN(PF_2)$_2$ (PNP),[11] cpRu(CO)$_2$Cl,[12] *fac*-ReBr(CO)$_3$(MeCN)$_2$,[13] Mo(CO)$_3$(CHT) (CHT = cyclohepta-1,3,5-triene),[14] Pt(C_2Ph_2)(PPh_3),[15] and IrCl(CO)(PPh_3)$_2$.[16] Other organometallic starting materials were purchased from Strem Chemicals. Proton and $^{31}P\{^1H\}$ NMR spectra were obtained on an IBM-Bruker AF-200 spectrometer at 200.132 and 81.015 MHz. Proton NMR spectra were additionally obtained on a GE Omega 400-MHz spectrometer at 400.082 MHz. All spectra were obtained at ambient probe temperature unless otherwise specified. Proton and phosphorus chemical shifts are respectively referenced to external tetramethylsilane (δ 0.0) and 85% H_3PO_4(δ 0.0) with positive shifts downfield of the reference. Infrared spectra were obtained on a Mattson-Cygnus 100 Fourier transform spectrometer using NaCl cells. All chromatographic separations were performed on 1.7 × 20 cm Florisil columns which were prepared in hexane under nitrogen. Photochemical reactions employed a Hanovia, 450-W, high-pressure mercury lamp and Pyrex reaction vessels. Microanalyses were performed by Galbraith Laboratories, Knoxville, TN.

(η^5-C_5H_5)RuCl(η^1-$CH_3N(PF_2)_2$)$_2$ (1). To a solution of 0.446 g (1.73 mmol) of cpRuCl(CO)$_2$ in 24 mL of hexane/dichloromethane (2:1, v/v) contained in a 50-mL Schlenk vessel topped by an ice-cooled condenser was added 0.72 g (4.33

® Abstract published in *Advance ACS Abstracts,* June 15, 1994.

(1) Stephan, D. W. *Coord. Chem. Rev.* **1989**, *95*, 41.
(2) Bullock, R. M.; Casey, C. P. *Acc. Chem. Res.* **1987**, *20*, 167.
(3) Chaudret, B.; Delavaux, B.; Poilblanc, R. *Coord. Chem. Rev.* **1988**, *86*, 191.
(4) Carr, S. W.; Fontaine, X. L. R.; Shaw, B. L.; Thornton-Pett, M. *J. Chem. Soc., Dalton Trans.* **1988**, 769 and references therein.
(5) Fontaine, X. L. R.; Jacobsen, G. B.; Shaw, B. L.; Thornton-Pett, M. *J. Chem. Soc., Dalton Trans.* **1988**, 741 and references therein.
(6) Blagg, A.; Pringle, P. G.; Shaw, B. L. *J. Chem. Soc., Dalton Trans.* **1987**, 1495 and references therein.
(7) Ferguson, G. S.; Wolczanski, P. T.; Parkanyi, L.; Zonnevylle, M. C. *Organometallics* **1988**, *7*, 1967.
(8) Mague, J. T; Johnson, M. P. *Organometallics* **1990**, *9*, 1254.
(9) Mague, J. T. *Organometallics* **1991**, *10*, 513.
(10) Mague, J. T.; Lin, Z. *Organometallics* **1992**, *11*, 4139.
(11) King, R. B.; Gimeno, J. *Inorg. Chem.* **1978**, *17*, 2390.
(12) Joseph, M. F.; Page, J. A.; Baird, M. C. *Organometallics* **1984**, *3*, 1749.
(13) Farona, M. F.; Kraus, K. F. *Inorg. Chem.* **1970**, *9*, 1700.
(14) King, R. B. *Organometallic Syntheses*: Academic Press: New York, 1965; Vol. 1, p 125.
(15) Blake, D. M.; Roundhill, D. M. *Inorg. Synth.* **1978**, *18*, 122.
(16) Blake, D. M.; Crabtree, R. H. *Inorg. Chem.* **1986**, *25*, 931.
(17) Key to NMR peak multiplicities: s, singlet; dd, doublet of doublets; dt, doublet of triplets; dm, doublet of multiplets; t, triplet; tm, triplet of multiplets; tt, triplet of triplets; m, multiplet, br, broad; br t, broad triplet.
(18) Key to infrared band intensities: vs, very strong; s, strong; m, medium, sh, shoulder.

0276-7333/94/2313-3027$04.50/0

mmol) of $MeN(PF_2)_2$. The solution was photolyzed for 0.75 h under a slow nitrogen purge during which time gas evolution occurred and a bright yellow solid formed. The resulting mixture was transferred to a clean flask and the solvent removed under reduced pressure. The product obtained initially is quite gummy but is transformed to a free-flowing powder by repeatedly scraping it from the walls of the flask, breaking up the lumps, and subjecting it to a dynamic vacuum for several hours (yield *ca.* 90%). The product showed no carbonyl absorptions, and its purity was sufficient for further reactions. The analytical sample was recrystallized from hexane/CH_2Cl_2 at −10 °C. Anal. Calcd for $C_7H_{11}N_2P_4F_8ClRu$: C, 15.70; H, 2.07; N, 5.23. Found: C, 16.3; H, 2.3; N, 4.8. ^1H NMR ($CDCl_3$): δ 5.09 (s, 5H, C_5H_5), 2.92 (m, 6H, N−CH_3).[17] $^{31}P\{^1H\}$ NMR ($CDCl_3$): δ(P_{Ru}) 165.0 (tm), δ 137.2 (tm).

(η^5-C_5H_5)Ru(P(O)F_2)(PF_2NHCH_3)$_2$ (2). A solution of **1** in 1 mL of dichloromethane was introduced onto a Florisil column, and the column was washed with dry hexane. Elution with acetonitrile that had not been *rigorously* dried removed a yellow band from which the solvent was removed under reduced pressure. Recrystallization of the residue from dichloromethane/diethyl ether afforded the product as yellow blocks in *ca.* 80% yield. Anal. Calcd for $C_7H_{13}P_3F_6N_2ORu$: C, 18.72; H, 2.92; N, 6.24. Found: C, 18.5; H, 2.8; N, 6.25. IR[18] (Nujol mull): 3295 (m) (ν_{N-H}), 1107 (vs) ($\nu_{P=O}$) cm^{-1}. ^1H NMR ($CDCl_3$): δ 5.24 (s, 5H, C_5H_5), 2.67 (dd (J = 11.6, 5.9 Hz), 6H N−CH_3). $^{31}P\{^1H\}$ NMR ($CDCl_3$): δ 167.2 (tm, PF_2NHMe), 117.5 (tt (^1J(P−F) = 1214, ^2J(P−P) = 87.4 Hz), $P(O)F_2$).

***fac*-ReBr(CO)$_3$(η^1-$CH_3N(PF_2)_2$)$_2$ (3).** To a solution of 0.2 g (0.46 mmol) of *fac*-$ReBr(CO)_3(MeCN)_2$ in 15 mL of dichloromethane was added 0.23 g (1.38 mmol) of $MeN(PF_2)_2$, and the solution was stirred for 14 h at room temperature. The solvent was removed in vacuo, and the resulting oil solidified after 3 h under a dynamic vacuum. The yield was virtually quantitative. The analytical sample was obtained by cooling a concentrated solution in hexane/dichloromethane at −10 °C. Anal. Calcd for $C_5H_6N_2P_4F_8O_3BrRe$: C, 8.78; H, 0.88; N, 4.10. Found: C, 9.0; H, 0.8; N, 3.5. IR (CH_2Cl_2 solution): 2087 (vs), 2035(2), 1968 (vs) cm^{-1} ($\nu_{C=O}$). ^1H NMR ($CDCl_3$): 2.95 (m, N−CH_3). $^{31}P\{^1H\}$ NMR ($CDCl_3$): δ 137.1 (tm), δ(P_{Re}) 121.3 (tm).

(η^5-C_5H_5)Ru(μ-$CH_3N(PF_2)_2$)$_2$Co(CO)$_2$ (4). Addition of 0.45 g (0.84 mmol) of **1** to a solution of 0.15 g (0.44 mmol) of $Co_2(CO)_8$ in 7 mL of toluene resulted in gas evolution and the formation of a green solid. After stirring at room temperature for 11 h, the mixture was filtered to give a clear brownish solution which was taken to dryness in vacuo. The resulting solid was taken up in 1 mL of CH_2Cl_2 and chromatographed. Initial elution with hexane removed a small yellow band which was not further characterized. Subsequent elution with hexane/CH_2Cl_2 (1:1, v/v) removed a large, orange yellow band from which orange crystals of the product were obtained following concentration under reduced pressure and cooling at −10 °C. (yield 0.43 g, 84%). Anal. Calcd for $C_9H_{11}P_4F_8N_2O_2RuCo$: C, 17.57; H, 1.81; N, 4.56. Found: C, 17.9; H, 2.0; N, 4.2. IR (CH_2Cl_2 solution): 2016 (vs), 1956 (s) cm^{-1} ($\nu_{C=O}$). ^1H NMR ($CDCl_3$): δ 5.07 (s, 5H, C_5H_5), 2.79 (m, 6H, N−CH_3). $^{31}P\{^1H\}$ NMR ($CDCl_3$): δ(P_{Ru}) 163.1 (tm), δ(P_{Co}) 169 (br).

***fac*-Re(CO)$_3$(μ-$CH_3N(PF_2)_2$)$_2$Co(CO)$_2$ (5).** Addition of 0.05 g (0.15 mmol) of $Co_2(CO)_8$ to 0.20 g (0.29 mmol) of **3** dissolved in 5 mL of toluene resulted in gas evolution and the formation of a green solid in a yellowish brown solution. After stirring at room temperature for 0.5 h, the solution was filtered and the solvent removed in vacuo to give a yellow brown oil. This was taken up in 2 mL of CH_2Cl_2 and diluted with 5 mL of hexane whereupon a white solid formed. This was filtered off, the filtrate taken to dryness in vacuo, and the yellow residue dissolved in 1 mL of CH_2Cl_2. On standing at −10 °C the product formed as large yellow crystals (yield 0.09 g, 43%). Anal. Calcd for $C_7H_6P_4F_8O_5N_2CoRe$: C, 1.67; H, 0.84; N, 3.90. Found: C, 1.2; H, 0.6; N, 3.9. IR (CH_2Cl_2 solution): 2074 (vs), 2021 (vs), 1972 (s), 1958 (sh) cm^{-1} ($\nu_{C=O}$). ^1H NMR ($CDCl_3$): δ 2.88 (m, N−CH_3). $^{31}P\{^1H\}$ NMR ($CDCl_3$): δ(P_{Co}) 160 (br, t), δ(P_{Re}) 128.2 (tm).

(η^5-C_5H_5)Ru(μ-$CH_3N(PF_2)_2$)$_2$IrCl$_2$($P(C_6H_5)_3$) (6). To a solution of 0.064 g (0.093 mmol) of $IrCl(CO)(PPh_3)_2$ in 7 mL of toluene was added 0.050 g (0.093 mmol) of **1**. After stirring for 21 h at room temperature, the solvent was removed from the cloudy yellow solution under reduced pressure and the residue was recrystallized from CH_2Cl_2/hexane at −10 °C to afford the product as yellow crystals (yield 0.08 g, 84%). The infrared spectrum showed no carbonyl absorptions. Anal. Calcd for $C_{25}H_{26}P_5F_8N_2Cl_2RuIr$: C, 29.28; H, 2.56. Found: C, 28.7; H, 2.5. ^1H NMR ($CDCl_3$): δ 7.77 (m), 7.33 (m) (15H, C_6H_5), 5.24 (s, 5H, C_5H_5), 2.70 (t (J = 7.6 Hz), 6H, N−CH_3). $^{31}P\{^1H\}$ NMR ($CDCl_3$): δ(P_{Ru}) 159.2 (tm), δ(P_{Ir}) 86.5 (tm), δ(PPh_3) −14.8 (m).

***fac*-Re(CO)$_3$(μ-$CH_3N(PF_2)_2$)$_2$IrBrCl($P(C_6H_5)_3$) (7).** To a solution of 0.189 g (0.274 mmol) of **3** in 5 mL of toluene was added 0.191 g (0.276 mmol) of $IrCl(CO)(PPh_3)_2$. After stirring for 15 h at room temperature a yellow solid had formed which was filtered off and washed with diethyl ether. Removal of free triphenylphosphine from the crude material proved difficult and a pure product was finally obtained by taking up the solid in 4 mL of dichloromethane, filtering the cloudy solution, diluting the filtrate with 3 mL of toluene, and crystallizing the product by the slow vapor diffusion of hexane into the resulting solution (yield 0.2 g, 62%). Anal. Calcd for $C_{23}H_{21}N_2O_3F_8P_5BrClReIr$: C, 23.47; H, 1.80; N, 2.38. Found: C, 24.0; H, 1.8; N, 2.4. IR (CH_2Cl_2 solution): 2076 (vs), 2029 (m), 1966 (s) cm^{-1} ($\nu_{C=O}$). ^1H NMR ($CDCl_3$): δ 7.82 (m), 7.38 (m) (15H, C_6H_5), 2.80 (br, 6H, N−CH_3). $^{31}P\{^1H\}$ NMR ($CDCl_3$): δ(P_{Re}) 124.8 (tm), δ(P_{Ir}) 84.0 (tm), δ(PPh_3) −21.7 (br).

(η^5-C_5H_5)Ru(μ-$CH_3N(PF_2)_2$)$_2$RhCl$_2$ (8). To a solution of 0.040 g (0.10 mmol) of $[RhCl(CO)_2]_2$ in 5 mL of toluene was added 0.116 g (0.217 mmol) of **1**. After stirring overnight at room temperature, an orange solid had precipitated which was filtered off and washed with diethyl ether. Recrystallization from CH_2Cl_2/diethyl ether afforded the product as red crystals (yield 0.12 g, 82%). The infrared spectrum indicated the absence of carbonyl absorptions. Anal. Calcd for $C_7H_{11}N_2P_4F_8Cl_2RhRu$: C, 12.47; H, 1.65; N, 4.16. Found: C, 12.6; H, 1.9; N, 4.0. ^1H NMR ($CDCl_3$): δ 5.45 (s, 5H, C_5H_5), 2.98 (br t, 6H, N−CH_3). $^{31}P\{^1H\}$ NMR ($CDCl_3$): δ(P_{Ru}) 163.3 (tm), δ(P_{Rh}) 128.2 (tm).

(η^5-C_5H_5)Ru(μ-$CH_3N(PF_2)_2$)$_2$RhCl$_2$($P(CH_3)_2C_6H_5$) (9). To a solution of 0.084 g (0.125 mmol) of **8** in 10 mL of dichloromethane/toluene (3:2, v/v) was added 0.17 g (0.125 mmol) of PMe_2Ph, and the solution was stirred overnight. Removal of the solvent from the clear orange solution in vacuo followed by recrystallization from dichloromethane/hexane afforded the product as orange crystals (yield 0.053 g, 52%). Anal. Calcd for $C_{15}H_{22}N_2P_5F_8Cl_2RuRh$: C, 22.18; H, 2.74. Found: C, 22.2; H, 2.7. ^1H NMR ($CDCl_3$): δ 7.38−7.64 (m, 5H, C_6H_5), 5.34 (s, 5H, C_5H_5), 2.78 (t (J = 7.4 Hz), 6H, N−CH_3), 1.95 (d (J = 10.8 Hz), 6H, P−CH_3). $^{31}P\{^1H\}$ NMR ($CDCl_3$): δ(P_{Ru}) 158.8 (tm), δ(P_{Rh}) 132.5 (tm), δ(PMe_2Ph) −19.5 (dm).

***fac*-Re(CO)$_3$(μ-$CH_3N(PF_2)_2$)$_2$RhClBr (10).** To a solution of 0.527 g (0.764 mmol) of **3** in 9 mL of toluene was added 0.150 g (0.386 mmol) of solid $[RhCl(CO)_2]_2$ whereupon vigorous gas evolution occurred and the solution became a cloudy orange color. After stirring for 16 h at room temperature, the bright yellow product was filtered off, washed with diethyl ether, and dried in vacuo (yield 0.40 g, 68%). Anal. Calcd for $C_5H_6N_2P_4F_8O_3ClBrRhRe$: C, 7.84; H, 0.79. Found: C, 7.5; H, 0.8. IR (Nujol mull): 2085 (s), 2029 (vs), 1975 (s) cm^{-1} ($\nu_{C=O}$). ^1H NMR (CD_3CN): δ 2.8 (br t, N−CH_3). $^{31}P\{^1H\}$ NMR ($(CD_3)_2CO$): δ 129.2 (tm), 127.7 (tm).

***fac*-Re(CO)$_3$(μ-$CH_3N(PF_2)_2$)$_2$PtBr($P(C_6H_5)_3$)·2CH_2Cl_2 (11).** To a solution of 0.190 g (0.275 mmol) of **3** dissolved in 5 mL of toluene was added 0.249 g (0.278 mmol) of $Pt(C_2Ph_2)(PPh_3)_2$. After stirring at room temperature for 21 h, the solvent was

Table 1. Summary of Crystallographic Data

	2	5	9	11
formula	$C_7H_{13}P_3F_6N_2ORu$	$C_7H_6F_8N_2O_5P_4CoRe$	$C_{15}H_{12}F_8N_2P_5Cl_2RuRh$	$C_{24}H_{23}F_8N_2O_3P_5BrCl_2RePt$
fw	449.18	718.08	812.09	1226.43
cryst size, mm	0.66 × 0.53 × 0.53	0.35 × 0.26 × 0.40	0.53 × 0.30 × 0.50	0.22 × 0.28 × 0.38
cryst syst	monoclinic	triclinic	monoclinic	monoclinic
space group	$P2_1/n$ (No. 14)	$P\bar{1}$ (No. 2)	$P2_1/c$ (No. 14)	$C2/m$ (No. 12)
a, Å	10.487(2)	9.794(1)	18.239(3)	12.649(2)
b, Å	11.832(2)	10.563(1)	8.195(2)	14.908(1)
c, Å	11.910(2)	9.624(2)	18.078(2)	19.798(2)
α, deg		98.06(1)		
β, deg	90.50(1)	101.29(1)	102.36(1)	96.600(9)
γ, deg		81.796(9)		
V, Å^3	1477.8(8)	959.9(4)	2639.4(8)	3709(2)
Z	4	2	4	4
ϱ_{calc}, g cm^{-3}	2.02	2.49	2.04	2.16
μ, cm^{-1}	14.2	76.7	17.5	86.1
range trans factors	0.4273–0.9806	0.4487–0.9986	0.7459–0.9993	0.6126–0.9995
temp, K	295	295	295	295
radtn	Mo Kα (graphite monochromated, λ = 0.710 73 Å)			
scan type	$\omega/2\theta$	$\omega/2\theta$	$\omega/2\theta$	$\omega/2\theta$
scan range, deg	0.8 + 0.34(tan θ)	0.8 + 0.2(tan θ)	0.8 + 0.34(tan θ)	0.8 + 0.2(tan θ)
2θ range, deg	1.0–52.0	1.0–52.0	1.0–50.0	1.0–52.0
total no. of refls	3220	3978	5169	3967
no. of unique refls	2895	3978	4644	3776
R_{int}	0.061		0.024	0.028
no. of obs data	2432 ($I \geq 3\sigma(I)$)	3586 ($I \geq 3\sigma(I)$)	4036 ($I \geq 3\sigma(I)$)	2928 ($I \geq 3\sigma(I)$)
no. of param	181	253	307	277
$(\Delta/\sigma)_{max}$ in last cycle	0.02	0.0	0.08	0.41
R^a	0.069	0.028	0.025	0.033
R^b	0.086	0.036	0.037	0.046
GOF^c	3.05	1.88	1.40	1.58
$\Delta\varrho$ in final ΔF map, e/Å^3	+2.47 to −2.30	+1.09 to −0.21	+0.81 to −0.51	+4.33 to −0.62

^{a} $R = \sum||F_o| - |F_c||/\sum|F_o|$. ^{b} $R_w = [\sum w(|F_o| - |F_c|)^2/\sum w(|F_o|)^2]^{1/2}$ with $w = 1/(\sigma_F)^2$; $\sigma_F = \sigma(F^2)/2F$; $\sigma(F^2) = [(\sigma_I)^2 + (0.04F^2)^2]^{1/2}$. ^{c} GOF = $[\sum w(|F_o| - |F_c|)^2/(N_o - N_v)]^{1/2}$ where N_o and N_v are, respectively, the number of observations and variables.

removed from the clear, yellow solution under reduced pressure to yield a yellow oil. This was taken up in dichloromethane and diluted with hexane. Upon cooling at −10 °C the product was obtained as yellow crystals (yield, 0.15 g, 42%). Anal. Calcd for $C_{25}H_{26}N_2O_3F_8P_5Cl_4BrRePt$: C, 22.90; H, 1.92; N, 2.14. Found: C, 22.5; H, 1.6; N, 1.8. IR (CH_2Cl_2 solution): 2074 (vs), 2029 (vs), 1968 (s) cm^{-1} ($\nu_{C\equiv O}$). ^{1}H NMR ($CDCl_3$): δ 7.67–7.34 (m, 15H, C_6H_5), 5.27 (s, 4H, CH_2Cl_2), 2.78 (br t, 6H, N–CH_3). ^{31}P{^{1}H} NMR ($CDCl_3$): $\delta(P_{Re})$ 122.9 (tm), $\delta(P_{Pt})$ 124.2 (tm), $\delta(PPh_3)$ −1.45 (m, ^1J(Pt–P) = 2402 Hz).

X-ray Crystallography. General procedures for crystal orientation, unit cell determination, and collection of intensity data on the CAD-4 diffractometer have been published.[19] All crystals were mounted on thin glass fibers and coated with epoxy cement to retard possible decomposition. The space groups for **2** and **9** were uniquely determined by the systematic absences in the final data sets. Raw intensities were corrected for Lorentz and polarization effects and for absorption using ψ scans on several reflections with χ near 90°. All structures except **9** were solved by Patterson methods and developed by successive cycles of full-matrix, least-squares refinement and $\Delta\varrho$ syntheses. The neutral atom scattering factors used include the real and imaginary corrections for the effects of anomalous dispersion.[20] In the late stages of the refinements, many of the hydrogen atoms present were evident in $\Delta\varrho$ maps. Except as noted below, these were placed in calculated positions (C–H = 0.95 Å) with isotropic thermal parameters 20% larger than those of the attached carbon atoms and updated periodically. All calculations were performed on a VAXstation 3100 computer with the MolEN suite of programs.[21] Crystallographic data pertinent to the present determination are presented in Table 1, final refined atomic parameters in Tables 2–5, and the remaining data as supplementary material.

Table 2. Positional Parameters (Esd) for cpRu(P(O)F$_2$)(PF$_2$NHMe)$_2$ (2)

atom	x	y	x	B_{eq}^a (Å^2)
Ru	0.19641(4)	0.20564(4)	−0.03900(4)	2.758(9)
P(1)	0.3834(2)	0.2914(1)	−0.0270(2)	3.58(3)
P(2)	0.2220(2)	0.1216(1)	0.1247(1)	3.08(3)
P(3)	0.2860(2)	0.0591(2)	−0.1286(1)	3.52(3)
F(1)	0.3881(5)	0.3926(4)	0.0574(6)	9.1(1)
F(2)	0.4160(5)	0.3656(6)	−0.1270(5)	11.4(1)
F(3)	0.2337(7)	0.2027(4)	0.2288(4)	7.7(2)
F(4)	0.0996(4)	0.0636(5)	0.1696(4)	7.6(1)
F(5)	0.3057(5)	0.0872(5)	−0.2557(3)	6.7(1)
F(6)	0.1847(4)	−0.0360(4)	−0.1510(4)	6.6(1)
O	0.4021(5)	0.0010(5)	−0.0913(4)	4.8(1)
N(1)	0.5152(6)	0.2316(5)	0.0013(6)	4.5(1)
N(2)	0.3277(6)	0.0300(5)	0.1529(5)	4.7(1)
C(1)	0.0841(8)	0.3649(6)	−0.0610(8)	5.9(2)
C(2)	0.0170(8)	0.2966(7)	0.0091(7)	5.8(2)
C(3)	−0.0153(7)	0.1990(7)	−0.0516(7)	4.8(2)
C(4)	0.0312(7)	0.2084(6)	−0.1592(6)	4.4(2)
C(5)	0.0951(8)	0.3118(7)	−0.1695(7)	5.3(2)
C(6)	0.6396(8)	0.2837(8)	0.0104(7)	5.7(2)
C(7)	0.3489(8)	−0.0247(7)	0.2595(6)	5.7(2)

^{a} Anisotropically refined atoms are given in the form of the isotropic equivalent displacement parameter defined as $B_{eq} = (8\pi^2/3)\sum_i\sum_j U_{ij}a^*_i a^*_j \mathbf{a}_i\cdot\mathbf{a}_j$.

(a) cpRu(P(O)F$_2$)(PF$_2$NHMe)$_2$ (2). The pale yellow crystal used for the data collection was cut from a large block that was obtained by cooling a dichloromethane/diethyl ether solution of the complex. Although somewhat larger than ideal, the tendency of the crystals to shatter when cut made it difficult to obtain a satisfactory fragment of smaller dimensions. The monoclinic cell indicated by the CAD-4 software was confirmed by the observation of 2/m diffraction symmetry. The intensity data were additionally corrected for a linear 2.1% decay in the intensities of the monitor reflections. The best crystal found still was of poor quality, as evidenced by the observation of rather broad and somewhat asymmetric dif-

(19) Mague, J. T.; Lloyd, C. L. *Organometallics* **1988**, *7*, 983.
(20) (a) Cromer, D. T.; Waber, J. T. *International Tables for X-ray Crystallography*; The Kynoch Press: Birmingham, England, 1974; Vol. IV, Table 2.2B. (b) Cromer, D. T. *Ibid.*, Table 3.2.1.
(21) Fair, C. K. MolEN, An Interactive Intelligent System for Crystal Structure Analysis, Enraf-Nonius, The Netherlands, 1990.

Table 3. Positional Parameters (Esd) for $Re(CO)_3(\mu\text{-}PNP)_2Co(CO)_2$(5)

atom	x	y	z	B_{eq}[a] (Å^2)
Re	0.21225(3)	0.23113(3)	0.37623(3)	2.770(5)
Co	0.14607(9)	0.27156(8)	0.07809(9)	2.59(2)
P(1)	0.2574(2)	0.0122(2)	0.3023(2)	3.76(4)
P(2)	0.2169(2)	0.0790(2)	0.0232(2)	3.32(4)
P(3)	0.3098(2)	0.3837(2)	0.1123(2)	3.04(4)
P(4)	0.4361(2)	0.2670(2)	0.3569(2)	3.01(4)
F(1)	0.3957(7)	−0.0609(5)	0.3779(6)	6.3(1)
F(2)	0.1573(7)	−0.0769(5)	0.3349(6)	7.1(1)
F(3)	0.3449(6)	0.0492(5)	−0.0562(6)	6.6(1)
F(4)	0.1189(7)	0.0017(5)	−0.0978(5)	6.9(2)
F(5)	0.3901(5)	0.3818(5)	−0.0152(5)	5.8(1)
F(6)	0.2807(6)	0.5338(4)	0.1359(7)	6.4(1)
F(7)	0.5255(6)	0.3312(5)	0.4956(5)	5.6(1)
F(8)	0.5476(5)	0.1506(5)	0.3303(6)	5.6(1)
O(1)	0.0256(9)	0.3176(7)	−0.2131(6)	6.7(2)
O(2)	−0.1099(6)	0.3866(7)	0.1756(7)	6.2(2)
O(3)	−0.0903(7)	0.1824(7)	0.3989(8)	6.9(2)
O(4)	0.320(1)	0.190(1)	0.6897(7)	8.7(3)
O(5)	0.1445(8)	0.5273(6)	0.4611(8)	6.2(2)
N(1)	0.2658(7)	−0.0350(5)	0.1349(7)	3.7(1)
N(2)	0.4513(6)	0.3625(6)	0.2420(6)	3.2(1)
C(1)	0.312(1)	−0.1700(8)	0.084(1)	6.4(3)
C(2)	0.5830(9)	0.4189(9)	0.247(1)	5.2(2)
C(3)	0.0740(9)	0.2995(8)	−0.0991(8)	4.1(2)
C(4)	−0.0088(8)	0.3371(8)	0.1458(8)	3.8(2)
C(5)	0.0183(9)	0.2011(9)	0.3873(9)	4.5(2)
C(6)	0.277(1)	0.2055(9)	0.5724(8)	4.9(2)
C(7)	0.1680(9)	0.4198(8)	0.4281(8)	4.2(2)

[a] Anisotropically refined atoms are given in the form of the isotropic equivalent displacement parameter defined as $B_{eq} = (8\pi^2/3)\sum_i\sum_j U_{ij}a^*_i a^*_j \mathbf{a}_i\cdot\mathbf{a}_j$.

Table 4. Positional Parameters (Esd) for $cpRu(\mu\text{-}PNP)_2RhCl_2$ (PMe_2Ph) (9)

atom	x	y	z	B_{eq}[a] (Å^2)
Rh	0.75148(1)	−0.01057(3)	0.47780(1)	2.018(4)
Ru	0.62136(1)	0.06821(3)	0.36299(1)	2.187(4)
Cl(1)	0.71283(5)	−0.2855(1)	0.49304(5)	3.68(2)
Cl(2)	0.82228(5)	−0.0975(1)	0.38382(5)	3.81(2)
P(1)	0.66219(4)	0.0837(1)	0.52771(4)	2.67(2)
P(2)	0.58159(4)	0.2688(1)	0.42076(4)	2.61(2)
P(3)	0.69840(4)	0.2312(1)	0.32287(4)	2.74(2)
P(4)	0.80007(4)	0.2236(1)	0.46259(4)	2.49(1)
P(5)	0.84707(5)	−0.0794(1)	0.58439(5)	2.92(2)
F(1)	0.6918(1)	0.1126(3)	0.6156(1)	4.32(5)
F(2)	0.5985(1)	−0.0340(3)	0.5400(1)	4.26(4)
F(3)	0.5894(1)	0.4524(2)	0.4007(1)	4.07(5)
F(4)	0.4960(1)	0.2810(3)	0.4210(1)	4.45(5)
F(5)	0.6646(1)	0.3894(3)	0.2799(1)	4.44(5)
F(6)	0.7342(1)	0.1697(3)	0.2570(1)	4.24(4)
f(7)	0.8861(1)	0.2292(3)	0.4694(1)	4.26(5)
F(8)	0.7971(1)	0.3590(2)	0.5215(1)	4.15(5)
N(1)	0.6209(1)	0.2672(3)	0.5112(1)	2.99(5)
N(2)	0.7705(1)	0.3189(3)	0.3815(1)	2.69(5)
C(1)	0.6098(2)	0.3879(5)	0.5690(2)	4.26(8)
C(2)	0.8109(2)	0.4630(5)	0.3615(2)	4.09(8)
C(3)	0.5615(2)	−0.1683(4)	0.3655(2)	4.09(8)
C(4)	0.5109(2)	−0.0540(5)	0.3264(2)	4.60(9)
C(5)	0.5362(2)	−0.0050(5)	0.2615(2)	4.64(9)
C(6)	0.6022(2)	−0.0945(5)	0.2605(2)	4.30(8)
C(7)	0.6183(2)	−0.1933(4)	0.3250(2)	3.92(8)
C(8)	0.8143(2)	−0.1832(5)	0.6602(2)	4.75(9)
C(9)	0.9144(2)	−0.2221(5)	0.5617(2)	4.91(9)
C(10)	0.9018(2)	0.0889(4)	0.6336(2)	2.91(6)
C(11)	0.8697(2)	0.1923(5)	0.6783(2)	3.85(8)
C(12)	0.9081(2)	0.3253(5)	0.7127(2)	4.61(9)
C(13)	0.9797(2)	0.3588(6)	0.7031(2)	4.93(9)
C(14)	1.0126(2)	0.2565(6)	0.6599(2)	4.79(9)
C(15)	0.9744(2)	0.1207(5)	0.6250(2)	3.57(7)

[A] Anisotropically refined atoms are given in the form of the isotropic equivalent displacement parameter defined as $B_{eq} = (8\pi^2/3)\sum_i\sum_j U_{ij}a^*_i a^*_j \mathbf{a}_i\cdot\mathbf{a}_j$.

fraction peaks, and this is also reflected in the rather high values of the final residuals. Despite this, most hydrogen atoms could be seen in a $\Delta\rho$ map following anisotropic

Table 5. Positional Parameters (Esd) for $Re(CO)_3(\mu\text{-}PNP)_2PtBr(PPh_3)\cdot CH_2Cl_2$ (11)

atom	x	y	z	B_{eq}[a] (Å^2)
Pt	0.16283(3)	0.000	0.28545(2)	2.253(6)
Re	0.23116(3)	0.000	0.43032(2)	3.91(1)
Br	−0.04453(8)	0.000	0.31266(6)	4.16(2)
P(1)	0.2149(2)	0.1400(1)	0.2917(1)	4.28(4)
P(2)	0.3485(2)	0.1140(2)	0.4133(1)	6.54(6)
P(3)	0.1031(2)	0.000	0.1683(1)	2.49(4)
F(1)	0.2508(4)	0.1772(3)	0.2245(3)	6.4(1)
F(2)	0.1303(5)	0.2148(4)	0.3008(4)	7.4(2)
F(3)	0.4698(5)	0.0958(7)	0.4100(5)	11.6(3)
F(4)	0.3656(6)	0.1872(5)	0.4689(3)	10.2(2)
O(1)	0.296(1)	0.026(2)	0.5831(6)	10.1(7)
O(2)	0.0650(7)	0.1485(6)	0.4450(4)	8.3(2)
N	0.3172(6)	0.1763(5)	0.3451(4)	7.1(2)
C(1)	0.271(1)	0.016	0.5254(6)	6.4(5)
C(2)	0.1238(7)	0.0933(7)	0.4378(4)	5.5(2)
C(3)	0.368(1)	0.2651(7)	0.3350(7)	11.1(3)
C(4)	0.049(1)	0.0998(8)	0.1328(6)	2.6(2)[b]
C(5)	0.086(1)	0.141(1)	0.0739(8)	4.0(3)
C(6)	0.037(2)	0.220(1)	0.0480(9)	5.0(4)
C(7)	−0.040(2)	0.260(1)	0.0816(9)	4.7(4)
C(8)	−0.0694(8)	0.2313(6)	0.1378(5)	5.2(2)
C(9)	−0.032(1)	0.145(1)	0.164(1)	3.6(2)[b]
C(4a)	−0.004(1)	0.086(1)	0.144(1)	2.6(2)[b]
C(5a)	−0.107(1)	0.058(1)	0.1165(9)	4.3(3)
C(6a)	−0.183(1)	0.122(1)	0.099(1)	5.8(4)
C(7a)	−0.163(1)	0.211(1)	0.1128(8)	4.8(3)
C(9a)	0.017(1)	0.175(1)	0.1558(8)	4.1(3)[b]
C(10)	0.206(1)	0.0362(8)	0.1123(7)	8.6(4)
C(11)	0.3114(8)	0.000	0.1330(6)	3.7(2)
C(12)	0.386(1)	0.005	0.0870(7)	6.6(4)
C(13)	0.358(1)	0.060(1)	0.0251(8)	4.2(3)
C(14)	0.257(1)	0.087(1)	0.0065(8)	4.3(3)
C(15)	0.176(1)	0.076(1)	0.0503(7)	3.6(3)
Cl(1s)	0.3482(7)	0.0843(5)	0.8122(4)	13.1(2)
Cl(2s)	0.4279(9)	0.0703(8)	0.7503(6)	14.2(3)
C(1s)	0.326(2)	0.000	0.751(1)	9.3(6)

[a] Anisotropically refined atoms are given in the form of the isotropic equivalent displacement parameter defined as $B_{eq} = (8\pi^2/3)\sum_i\sum_j U_{ij}a^*_i a^*_j \mathbf{a}_i\cdot\mathbf{a}_j$. [b] Atoms refined isotropically.

refinement of the non-hydrogen atoms. These included one attached to N(2) (H(2n)). This would not refine satisfactorily and so was included as a fixed contribution in the position indicated by the $\Delta\rho$ map. Because the map was rather noisy, it was less certain whether there was also a hydrogen attached to N(1) or if there was one attached to the oxygen atom on P(3). Small peaks appeared in positions that were reasonably consistent with both choices, but the position of that near N(1) seemed somewhat more reasonable, and on the basis of spectroscopic arguments (see Discussion), we feel that this is the correct choice. This atom, H(1n), was thus treated as was H(2n). The significant features remaining in the final $\Delta\rho$ map are close to the Ru atom and are considered to be artifacts resulting from the poor quality of the crystal and possibly inadequacies of the empirical absorption correction.

(b) *fac*-$Re(CO)_3(\mu\text{-}MeN(PF_2)_2)_2Co(CO)_2$ (5). The golden yellow crystal used was cut from a larger sample which had been crystallized from hexane/dichloromethane. No higher symmetry cell than the triclinic cell obtained by the CAD-4 software could be found, and the choice of $P\bar{1}$ as the correct space group, as suggested by intensity statistics, was confirmed by the successful refinement. The intensity data were additionally corrected for an anisotropic 4.9% decline in the intensities of the intensity monitors. The refinement converged without difficulty and the final $\Delta\rho$ map was essentially featureless.

(c) $cpRu(\mu\text{-}MeN(PF_2)_2)_2RhCl_2(PMe_2Ph)$ (9). The orange crystal used was cut from a larger sample which had been crystallized from a concentrated dichloromethane/hexane solution. The monoclinic cell obtained by the CAD-4 software was confirmed by the observation of 2/*m* diffraction symmetry, and the space group was uniquely determined by the systematic

absences observed in the final data set. The intensity data were additionally corrected for a 1.6% linear decay in the intensity of the intensity monitors. The locations of the metal atoms were obtained by direct methods (SIR-88),[22] and the development and refinement of the model was uneventful. The final $\Delta\rho$ map was essentially featureless.

(d) *fac*-$Re(CO)_3(\mu\text{-}MeN(PF_2)_2)_2PtBr(PPh_3)\cdot CH_2Cl_2$ (11). The yellow crystal used for the data collection was obtained by layering a dichloromethane solution of the complex with hexane and cooling to −10 °C. The monoclinic cell indicated by the CAD-4 software was confirmed by the observation of 2/*m* diffraction symmetry, and inspection of a limited data set showed the systematic absence $h + k = 2n + 1$ indicative of a C-centered cell. The data set was collected in the quadrant $h,k,\pm l$ using the condition $h + k = 2n$, and no further systematic absences were seen, indicating the possible space groups to be *C*2, *Cm*, or *C*2/*m*. A linear decay correction was applied to compensate for a 5.5% decrease in the intensities of the check reflections. Inspection of the Patterson function showed it to be consistent only with *C*2 or *C*2/*m*, and since a reasonable density indicated $Z = 4$, the solution was initially attempted in *C*2. While this revealed the majority of the structure, two of the phenyl rings appeared disordered, the P—N distances were not uniform and there were large (>0.6) correlations between the *x* and *z* coordinates of the phosphorus and fluorine atoms of the $MeN(PF_2)_2$ ligands. This last observation suggested that these atoms were related by symmetry so the refinement was continued in the centric space group *C*2/*m* with Re, Pt, Br, and P(3) on the mirror plane. This significantly improved the uniformity of the P—N distances but the triphenylphosphine ligand remained disordered about the mirror and it wsa also evident that the axial carbonyl group (C(1)—O(1)) lay just off the mirror. In this model, the majority of the phenyl carbon atoms and O(1) were well-resolved and a series of $\Delta\rho$ maps were used to determine reasonable positions for C(1) and the remaining phenyl carbon atoms from the overlapping images. The final refinement involved alternate cycles varying first anisotropic thermal parameters and then positional parameters for C(1). Also the overlapping phenyl carbon atoms were alternately refined with isotropic thermal parameters. A molecule of dichloromethane was also located, which is disordered over two sites in the mirror plane with occupancies, determined by trial refinements of occupancy parameters, of 0.6 and 0.4. In the final cycle, all parameters had $\Delta/\sigma < 0.1$ except for one thermal parameter of a disordered carbon atom. The residual density seen in the final $\Delta\rho$ was well-removed from the rest of the atoms located and is presumed to be due to an additional solvent molecule, but no satisfactory model could be devised. Despite the disorder required by the choice of *C*2/*m* as the space group, we feel that this is correct for the following reasons: (1) It proved impossible to satisfactorily locate all the phenyl carbon atoms in *C*2; (2) The final, refined P—N distances are much more reasonable in *C*2/*m*; (3) Attempted refinement of both enantiomers in *C*2 led to large correlations between parameters of atoms which would be symmetry-related in *C*2/*m*; (4) Although the intensity statistics did not provide a clear choice between the centric and acentric space groups, there is a slight bias toward the former.

Results and Discussion

Synthesis of Complexes. Photolysis of a hexane/dichloromethane solution of $cpRuCl(CO)_2$ in the presence of excess $MeN(PF_2)_2$ readily yields a yellow, crystalline material analyzing as $cpRuCl(MeN(PF_2)_2)_2$ (**1**). The $^{31}P\{^1H\}$ NMR spectrum consists of two complex reasonances of equal intensity, the higher field of which is close to the chemical shift of the free ligand. This

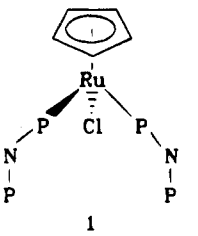

1

and the observation of a single resonance for the ligand methyl groups, the 6:5 ratio of the intensity of this resonance to that for the cyclopentadienyl group, and the absence of carbonyl absorptions in the infrared spectrum are all consistent with the formulation $cpRuCl(\eta^1\text{-}MeN(PF_2)_2)_2$, the ruthenium analog of $cpFeCl(\eta^1\text{-}MeN(PF_2)_2)_2$.[11] In contrast to the synthesis employed for the iron complex, attempts to prepare **1** thermally led to incomplete substitution of carbon monoxide. Although stable under nitrogen, **1** appears more moisture-sensitive than its iron analog and cleavage of the $MeN(PF_2)_2$ ligand by traces of water and/or acid is relatively facile. This was indicated by observing in some preparations of **1**, and in the products of some reactions of **1** that were incomplete and had been subjected to chromatographic workup, ^{31}P resonances incompatible with species containing intact $MeN(PF_2)_2$ ligands. To verify this, a pure sample of **1** was chromatographed on Florisil and eluted with acetonitrile which had not been rigorously dried. This afforded yellow crystals of a material having the same ^{31}P NMR spectrum as that originally seen for the impurity in **1**. A crystal structure determination indicated its formulation as $cpRu(P(O)F_2)(PF_2NHMe)_2$ (**2**) and the elemental

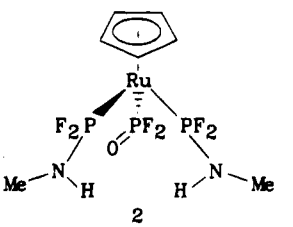

2

analysis obtained agrees well with this composition. In the formation of **2** from **1**, both $MeN(PF_2)_2$ ligands have been cleaved and the chloride replaced by a difluorophosphoryl ligand. As only one hydrogen attached to nitrogen could be located with confidence (vide infra), the X-ray study does not unequivocally distinguish between the formulations $cpRu(P(O)F_2)(PF_2NHMe)_2$ and $cpRu(P(OH)F_2)(PF_2{=}NMe)(PF_2NHMe)$ but we believe the spectroscopic data support the former. In particular, only a single chemical shift is observed for the ligand methyl groups and only two phosphorus resonances are evident in a 2:1 intensity ratio. Were the latter formulation to be correct, different chemical shifts for the phosphorus atoms of $PF_2{=}NMe$ and PF_2NHMe ligands could be expected and their methyl groups may have different chemical shifts as well. Unfortunately, no resonances for N—H groups could be confidently identified. The infrared spectrum shows a strong, sharp band at 1107 cm^{-1} which, although distinctly lower in energy than that found for $\nu_{P=O}$ in $PtCl(P(O)F_2)(PPh_3)_2$ (1247 cm^{-1})[10] and related species (1206−1252 cm^{-1}),[23] is

(22) Burla, M. C.; Camalli, M.; Cascarano, G.; Giacovazzo, C.; Polidori, G.; Spagna, R.; Viterbo, D. *J. Appl. Crystallogr.* **1989**, *22*, 389.

(23) Grosse, J.; Schmutzler, R. *J. Chem. Soc., Dalton Trans.* **1976**, 405.

neverthelessconsiderably higher than the range associated with P—OH stretching vibrations (1040–909 cm^{-1}).[24] We therefore believe this band should be assigned to $\nu_{P=O}$, and although the X-ray data suggest that intramolecular N—H- - -O=P hydrogen bonding is not strong, there may be sufficient interaction to cause the observed lowering.

Facile displacement of acetonitrile from *fac*-$ReBr(CO)_3(MeCN)_2$ occurs in the presence of excess $MeN(PF_2)_2$ on prolonged reaction in dichloromethane solution, and high yields of a white, crystalline product analyzing as $ReBr(CO)_3(MeN(PF_2)_2)_2$ (**3**) are obtained.

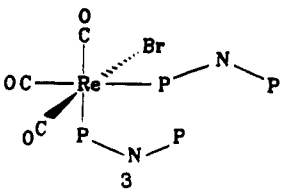

3

The three band pattern in the carbonyl stretching region of the infrared spectrum of **3** is very similar to that of the starting material, indicating retention of *fac* stereochemistry about rhenium. The $^{31}P\{^1H\}$ NMR spectrum shows two complex reasonances of equal intensity, the lower field of which has virtually the same chemical shift as that assigned to the uncoordinated end of the $MeN(PF_2)_2$ ligand in **1**. This together with the observation of a single resonance for the ligand methyl groups is consistent with the formulation of **3** as *fac*-$ReBr(CO)_3(\eta^1\text{-}MeN(PF_2)_2)_2$. In the crude product, a weak resonance at δ 86.5 having an appearance similar to the $X_2AA'X'_2$ pattern of the free ligand is frequently seen. The species giving this resonance is also the major product after reaction times of *ca.* 1 h, and it can be converted to **3** by extended reaction with excess $MeN(PF_2)_2$. The significant upfield shift of this phosphorus resonance compared with that for the coordinated phosphorus atom in **3** (δ 121.3) is consistent with the presence of a chelating $MeN(PF_2)_2$ ligand. We presume this species is *fac*-$ReBr(CO)_3(\eta^2\text{-}MeN(PF_2)_2)$, analogous to *fac*-$ReBr(CO)_3(\eta^2\text{-dmpm})$ (dmpm = bis(dimethylphosphino)methane) which has been prepared by the same route,[25] but it has not been characterized further.

The reaction of **1** and **3** with a variety of low-valent metal complexes has been investigated for the synthesis of heterobimetallic complexes. As observed previously for $cpFeCl(\eta^1\text{-}MeN(PF_2)_2)_2$,[10] these reactions generally proceed with transfer of halide from ruthenium or rhenium to the low-valent metal. Thus, for example, immediate gas evolution occurs when **1** and **3** are treated with $Co_2(CO)_8$ and precipitates of the respective Co(II) halides form. From the respective filtrates could be isolated orange and yellow, crystalline products which analyze for $cpRuCo(CO)_2(MeN(PF_2)_2)_2$ (**4**) and $ReCo(CO)_5(MeN(PF_2)_2)_2$ (**5**). The infrared spectrum of **4** shows two strong carbonyl bands at energies comparable to those found in $cpFe(\mu\text{-}MeN(PF_2)_2)_2Co(CO)_2$,[10] while the $^{31}P\{^1H\}$ NMR spectrum shows a complex resonances at virtually the same chemical shift as that assigned to the coordinated phosphorus in **1** together with a broad resonance at a slightly lower field which

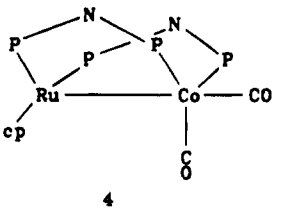

4

approximates a triplet. These are assigned, respectively, to phosphorus coordinated to ruthenium and to cobalt, with the breadth of the latter attributed to the presence of the cobalt nuclear quadrupole. All the data are consistent with the formulation of **4** as $cpRu(\mu\text{-}MeN(PF_2)_2)_2Co(CO)_2$ with a structure analogous to its iron analog.[10]

The infrared spectrum of **5** in the carbonyl region can be interpreted as an overlap of the patterns expected for {*fac*-$Re(CO)_3$} and {*cis*-$Co(CO)_2$} moieties, and the

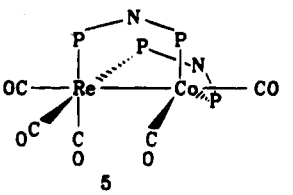

5

$^{31}P\{^1H\}$ NMR spectrum indicates the presence of equivalent bridging $MeN(PF_2)_2$ ligands, with the resonance assigned to phosphorus on cobalt again being quite broad. The data are thus in accord with formulation of **5** as *fac*-$Re(CO)_3(\mu\text{-}MeN(PF_2)_2)_2Co(CO)_2$, and this has been confirmed by an X-ray crystal structure determination.

Reaction of **1** and **3** with $IrCl(CO)(PPh_3)_2$ occurs more slowly, and yellow, crystalline products can be obtained which analyze respectively as $cpRuIrCl_2(MeN(PF_2)_2)_2(PPh_3)$ (**6**) and $ReIrBrCl(CO)_3(MeN(PF_2)_2)_2(PPh_3)$ (**7**).

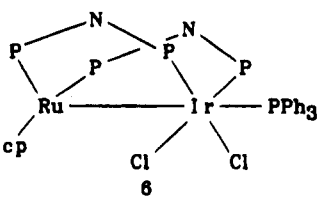

6

The $^{31}P\{^1H\}$ NMR spectrum of **6** shows three resonances of relative intensity 2:2:1 in the order of increasing field. The first two are the typical complex triplets seen for the bridging $MeN(PF_2)_2$ ligand with the lowest field one at a chemical shift comparable to those seen for the ruthenium-bound phosphorus atoms in **1** and **4** while the other is close to that found for the phosphorus coordinated to iridium in $cpFe(\mu\text{-}MeN(PF_2)_2)_2IrCl_2(PMe_2Ph)$.[9] The upfield resonance can be assigned to the triphenylphosphine ligand bound to iridium. No evidence for the presence of a carbonyl ligand could be seen in the infrared spectrum and we therefore formulate **6** as $cpRu(\mu\text{-}MeN(PF_2)_2)_2IrCl_2(PPh_3)$ with a structure like that of the Fe/Ir complex cited just above.[9]

Purification of **7** proved troublesome and this is presumably at least partly responsible for the rather low yield. It is also possible that some redistribution of bromide and chloride ligands occurred during the initial reaction and/or workup, but the analytical data agree quite favorably with the proposed formulation so

(24) Bellamy, L. J. *The Infrared Spectra of Complex Molecules*, 3rd ed.; Halsted Press: New York, 1975; Vol. 1, Chapter 18.
(25) Magne, J. T. *Inorg. Chem.*, submitted for publication.

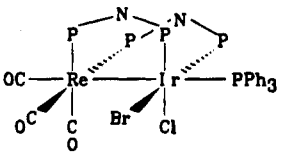

7

we feel reasonably confident that the isolated product is the mixed chloro/bromo species. The $^{31}P\{^1H\}$ NMR spectrum shows complex triplet resonances at chemical shifts comparable to those seen for the rhenium-bound phosphorus in **3** and **5** and for the iridium-bound phosphorus of $MeN(PF_2)_2$ in **6**. These are of equal relative intensities, and each is twice the intensity of the highest field resonance which is assigned to triphenylphosphine on iridium. The resonance assigned to $MeN(PF_2)_2$ on iridium is broader and more complex in appearance than the corresponding signal in **6** which is consistent with a slight nonequivalence of the two $-PF_2$ groups that could be expected on the basis of the proposed structure. The carbonyl region of the infrared spectrum is fully consistent with the presence of the {*fac*-$Re(CO)_3$} moiety and does not indicate that any additional carbonyl ligands are present. We therefore propose that **7** be formulated as *fac*-$Re(CO)_3(\mu$-$MeN(PF_2)_2)_2IrBrCl(PPh_3)$. In both **6** and **7** the presence of a metal—metal bond is proposed to be consistent with their observed diamagnetism. Without crystal structure determinations it is not possible to say whether this results from formation of a formal single bond or from a relatively weak coupling of unpaired electrons between the metals, but on the basis of the structural data available here and from previous work[9,10] it is likely that the metal—metal interaction is weak.

Combination of **1** and $[RhCl(CO)_2]_2$ yields red crystals of a product showing no bands in the carbonyl region and analyzing as cpRuRhCl$_2$(MeN(PF$_2$)$_2$)$_2$ (**8**). The

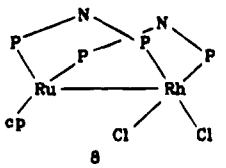

8

proton and phosphorus NMR spectra are very similar in appearance, apart from the chemical shift of the downfield resonance in the latter spectrum, to those obtained previously for cpFe(μ-MeN(PF$_2$)$_2$)$_2$RhCl$_2$,[9] indicating that **8** should be similarly formulated.

Complex **8** reacts rapidly with 1 equiv of dimethylphenylphosphine and the orange, crystalline product obtained analyzes for cpRuRhCl$_2$(MeN(PF$_2$)$_2$)$_2$(PMe$_2$Ph) (**9**). The $^{31}P\{^1H\}$ NMR spectrum in the low-field region

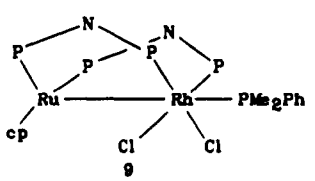

9

closely resembles that of **8**, while a new resonance appearing as a doublet of multiplets occurs upfield and is assigned to dimethylphenylphosphine coordinated to rhodium. This and the ^1H NMR data quoted in the Experimental Section suggest **9** be formulated as cpRu(μ-MeN(PF$_2$)$_2$)$_2$RhCl$_2$(PMe$_2$Ph), and this has been confirmed by an X-ray crystal structure analysis.

Initially, it was attempted to prepare **9** from the reaction of **1** with RhCl(CO)(PMe$_2$Ph)$_2$ by analogy with the route used for **6**. Indeed, moderate amounts of **9** are formed but this reaction is considerably more complex. When followed by ^{31}P NMR in toluene/deuteriobenzene solution, all of the starting materials appear to be consumed within 0.5 h and a substantial amount of **9** is also present. Additional species are indicated by a pair of triplets of multiplets which overlap the signals due to the MeN(PF$_2$)$_2$ ligands in **9** and by two pairs of upfield resonances, each pair of which consists of a doublet of triplets and a doublet of doublets in a 1:2 intensity ratio. The low-field resonances are tentatively identified as those of cpRu(P(O)F$_2$)(PF$_2$NHMe)$_2$ (**2**), while the upfield ones are attributed to *cis-mer*-RhHCl$_2$(PMe$_2$Ph)$_3$ and *mer*-RhCl$_3$(PMe$_2$Ph)$_3$ by comparison with the spectra of authentic samples. Thus, the upfield signals predominating after 0.5 h [δ 19.7 (dt (^1J(Rh—P) = 136.9, ^2J(P—P) = 29.5 Hz)), 1.8 (dd (^1J(Rh—P) = 95.1, ^2J(P—P) = 29.5 Hz))] are virtually the same as for the major species obtained from the reaction of a slight excess of HCl with RhCl(PMe$_2$Ph)$_3$[26] [δ 19.6 (dt (^1J(Rh—P) = 135.8, ^2J(P—P) = 29.5 Hz)), 1.83 (dd (^1J(Rh—P) = 95.0, ^2J(P—P) = 29.5 Hz)), C_6D_6 solution]. This latter material also shows a high-field proton resonance at δ −16.1 as a poorly-resolved, overlapping doublet of triplets having coupling constants of approximately 13 and 30 Hz. These data are consistent with the species being *cis-mer*-RhHCl$_2$(PMe$_2$Ph)$_3$, although the reported NMR data on this complex are sketchy.[26b] Over time, the ^{31}P resonances attributed to *cis-mer*-RhHCl$_2$(PMe$_2$Ph)$_3$ decay to be replaced by the second pair of high-field resonances, and after 6 h, only the latter are seen, while the amount of **9** appears not to have changed. The remaining high-field resonances appear at δ 1.3 (dt (^1J(Rh—P) = 112.6, ^2J(P—P) = 25.2 Hz)) and −6.0 (dd (^1J(Rh—P) = 85.3, ^2J(P—P) = 25.2 Hz)) and are also seen as the minor species formed in the reaction of HCl with RhCl(PMe$_2$Ph)$_3$ described above. The chemical shifts and coupling constants from both spectra agree well with those reported for *mer*-RhCl$_3$(PMe$_2$Ph)$_3$ when account is taken of the different solvent used in the earlier report.[27] The independent observation that **9** is not disrupted by the presence of excess PMe$_2$Ph over comparable periods of time suggests that the Rh(III) side products seen in the reaction under discussion are not formed from **9**. The presence of **2** indicates that some hydrolysis of **1** has occurred, presumably by traces of moisture in the solvent, and this could be expected to generate HCl. The observation of *cis-mer*-RhHCl$_2$(PMe$_2$Ph)$_3$ early in the reaction and its subsequent conversion to *mer*-RhCl$_3$(PMe$_2$Ph)$_3$ is consistent with this since the hydride complex is known to react with HCl to form the trichloride complex.[26] Moreover the presence of the hydride complex suggests prior formation of RhCl(PMe$_2$Ph)$_3$, from which the hydride could be obtained by oxidative addition of HCl. As the formation of **9** requires displacement of the

(26) (a) Intille, G. M. *Inorg. Chem.* **1972**, *11*, 695. (b) Betts, C. E.; Haszeldine, R. N.; Parish, R. V. *J. Chem. Soc., Dalton Trans.* **1975**, 2215. (c) The $^{31}P\{^1H\}$ NMR spectrum (C_6D_6) of RhCl(PMe$_2$Ph)$_3$ is δ 12.1 (dt (^1J(Rh—P) = 181.1, ^2J(P—P) = 45.3 Hz)) and δ −0.15 (dd (^1J(Rh—P) = 134.0, ^2J(P—P) = 45.3 Hz)).

(27) Mann, B. E.; Masters, C.; Shaw, B. L. *J. Chem. Soc., Dalton Trans.* **1972**, 704.

carbonyl and one phosphine ligand from RhCl(CO)-$(PMe_2Ph)_2$, and as this undoubtedly occurs in a stepwise fashion, we suggest that **A** (L = PMe_2Ph) is a plausible

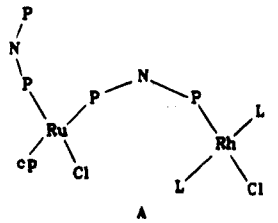

A

intermediate. Once some **9** has formed, there will also be free PMe_2Ph present and this could react with **A** to regenerate **1** and form $RhCl(PMe_2Ph)_3$. Other pathways are certainly possible, but this appears to be the most straightforward.

Complex **3** readily reacts with $[RhCl(CO)_2]_2$ to form a bright yellow, rather insoluble powder which analyzes for $Re(CO)_3(MeN(PF_2)_2)_2RhClBr$ (**10**). The infrared

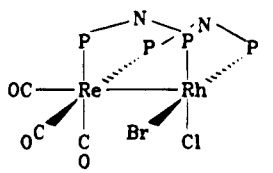

10

spectrum shows only three carbonyl absorptions which is consistent with the presence of the {*fac*-$Re(CO)_3$} moiety. The low solubility of the complex made it difficult to obtain good NMR spectra but it appeared from the proton spectrum that only one ligand methyl resonance was present, indicating the $MeN(PF_2)_2$ ligands to be equivalent. The $^{31}P\{^1H\}$ NMR spectrum had a very poor signal to noise ratio even after extended scan times but is best described as two closely overlapping triplets of multiplets with chemical shifts close to those found for the Re-bound $MeN(PF_2)_2$ ligands in **7** and the rhodium-bound ones in **8**. Formulation of **10** as *fac*-$Re(CO)_3(\mu$-$MeN(PF_2)_2)_2RhClBr$ is thus indicated.

Complex **3** also reacts with $Pt(C_2Ph_2)(PPh_3)_2$ to yield yellow crystals analyzing as $Re(CO)_3(MeN(PF_2)_2)_2PtBr(PPh_3)\cdot 2CH_2Cl_2$ (**11**) after crystallization from hexane/

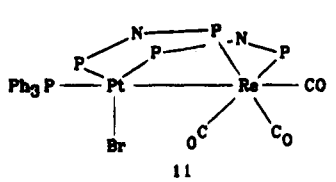

11

dichloromethane. The infrared spectrum shows three carbonyl bands attributable to the {*fac*-$Re(CO)_3$} moiety, while the proton NMR shows a single resonance for the ligand methyl protons as well as resonances in the aromatic region and for the solvent dichloromethane. The $^{31}P\{^1H\}$ NMR consists of two, substantially overlapped, low-field triplet of multiplet resonances having apparent equal intensities and a high-field multiplet with platinum satellites. From these data we formulate **11** as *fac*-$Re(CO)_2(\mu$-$MeN(PF_2)_2)_2PtBr(PPh_3)\cdot 2CH_2Cl_2$, and this has been confirmed by an X-ray structure study.

Miscellaneous Reactions. The reaction of **1** with $Pt(C_2Ph_2)(PPh_3)_2$ appears to proceed in an analogous fashion to that found previously for cpFeCl(η^1-$MeN(PF_2)_2)_2$.[10] Thus the $^{31}P\{^1H\}$ NMR spectrum of the crude reaction mixture clearly shows reasonances attributable to *trans*-$PtCl(P(O)F_2)(PPh_3)_2$[10] together with a set of resonances of approximately equal intensities at δ 255.9, 201.5, 187.3, and 27.7. The first appears as a triplet of doublets of doublets with platinum satellets (^1J(P—F) = 1151, ^1J(Pt—P) = 4014, J(P—P) = 21.2 Hz), while the second and third are complex triplets of multiplets with no satellites. The last is a multiplet and also possesses platinum satellites (^1J(Pt—P) = 3447 Hz). The overall pattern is qualitatively similar to that observed for cpFe(PF_2NHMe)(μ-PF_2NMe)(μ-PF_2)PtCl(PPh_3) which is the second major product obtained from cpFeCl(η^1-$MeN(PF_2)_2)_2$ and $Pt(C_2Ph_2)(PPh_3)_2$[10] and suggests that the analogous cpRu(PF_2NHMe)(μ-PF_2NMe)(μ-PF_2)Pt-(PPh_3) is found here. Because of the similarity to the Fe/Pt system described earlier, this reaction was not pursued further.

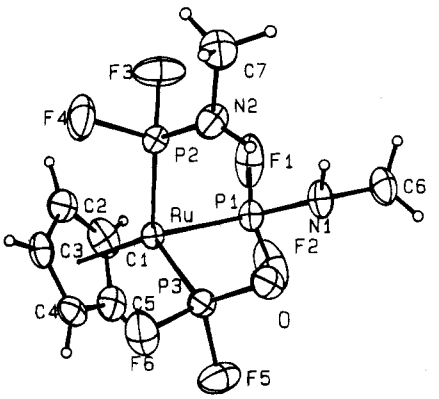

Figure 1. Perspective view of cpRu($P(O)F_2$)($PF_2NHMe)_2$ (**2**). Thermal ellipsoids are drawn at the 30% probability level except for the hydrogen atoms which are of arbitrary size of clarity.

Reaction of either **1** or **3** with $Ni(CO)_2(PPh_3)_2$ produces a darkening in the color of the solution whether performed at 25 or 60 °C, but the $^{31}P\{^1H\}$ NMR spectra of the crude reaction mixtures indicate that most of the $Ni(CO)_2(PPh_3)_2$ remained unchanged while the downfield region showed only weak and ill-defined resonances. We conclude that **1** and **3** are largely unreactive toward $Ni(CO)_2(PPh_3)_2$ under these conditions and decompose in the course of the experiment.

Description of Structures. (a) cpRu($P(O)F_2$)(PF_2-$NHMe)_2$ (2). A perspective view of **2** is shown in Figure 1, while pertinent bond distances and interbond angles appear in Table 6. The shortest intra- and intermolecular contacts are respectively O- - -H(2n) = 2.45 and O- - -H(1n) = 2.43 Å, but these are both sufficiently long such that strong N—H- - -O hydrogen bonding is unlikely. As noted in the Experimental Section, a hydrogen atom attached to N(2) could be located with confidence but the poor quality of the data set made it difficult to be certain whether or not N(1) should also bear a hydrogen atom. In addition, there appeared a comparably sized peak in the $\Delta\rho$ map which was in a plausible position to indicate the presence of a hydrogen attached to oxygen. The observed diamagnetism of **2** indicates it to be a Ru(II) species so that only one of the phosphorus-containing ligands can formally be uninegative, so this uncertainty about the position of a second hydrogen atom corresponds to an uncertainty

Table 6. Bond Distances (Å) and Interbond Angles (deg) for cpRu(P(O)F$_2$)(PF$_2$NHMe)$_2$ (2)[a]

	Distances		
Ru—P(1)	2.211(2)	Ru—C(5)	2.254(7)
Ru—P(2)	2.203(2)	P(1)—N(1)	1.586(7)
Ru—P(3)	2.247(2)	P(2)—N(2)	1.584(6)
Ru—C(1)	2.237(7)	P(3)—F(5)	1.566(5)
Ru—C(2)	2.248(8)	P(3)—F(6)	1.568(5)
Ru—C(3)	2.225(8)	P(3)—O	1.463(5)
Ru—C(4)	2.235(7)		
	Angles		
P(1)—Ru—P(2)	92.92(7)	Ru—P(2)—N(2)	125.1(2)
P(1)—Ru—P(3)	90.55(7)	Ru—P(3)—O	124.7(2)
P(1)—Ru—C′[b]	124.63(7)	Ru—P(3)—F(5)	110.8(2)
P(2)—Ru—P(3)	91.43(6)	Ru—P(3)—F(6)	110.4(2)
P(2)—Ru—C′[b]	123.81(7)	F(5)—P(3)—O	106.0(3)
P(3)—Ru—C′[b]	123.84(7)	F(6)—P(3)—O	105.9(3)
Ru—P(1)—N(1)	125.4(3)	F(5)—P(3)—F(6)	94.8(3)

[a] Numbers in parentheses are estimated standard deviations in the least significant digit. [b] C′ is the centroid of the cyclopentadienyl ring.

between the formulations cpRu(P(O)F$_2$)(PF$_2$NHMe)$_2$ and cpRu(P(OH)F$_2$)(PF$_2$=NMe)(PF$_2$NHMe). We feel confident in our choice of the former, despite this uncertainty, based on the spectroscopic data discussed earlier and on the observed geometry of the ligand assigned the formulation P(O)F$_2$. The thermal parameters of F(5), F(6), and O are well-behaved and indicate that the P(O)F$_2$ moiety is not rotationally disordered. The P(3)—O distance of 1.463(5) Å compares well with the value of 1.471(17) Å found for the corresponding distance in *trans*-PtCl(P(O)F$_2$)(PEt$_2$Ph)$_2$.[28] It is also comparable to the P—O distances in other formally P=O moieties, for example 1.469(4) Å to the terminal oxygen in (PhCH$_2$O)$_2$P(O)OH.[29] By contrast the P—OH distance in this last compound is 1.545(4) Å. The remaining geometry of the P(O)F$_2$ ligand also compares favorably with that found in the platinum complex cited above. Furthermore, the P—N distances and Ru—P—N angles in the other two ligands in **2** are equivalent within experimental error and compare favorably with those found previously for the PF$_2$NHMe ligands in cpFe(PF$_2$NHMe)(μ-PF$_2$NMe)(μ-PF$_2$)PtCl(PPh$_3$) (1.589(8) Å, 124.3(3)°)[10] and in Mo$_2$(CO)$_3$(PF$_2$NHMe)(μ-PF$_2$)(μ-Cl)-(μ-MeN(PF$_2$)$_2$)$_2$ (1.593(3) Å, 123.21(1)°).[30] It should be mentioned that in the one complex proposed to contain a terminal [MeN=PF$_2$]$^-$ ligand, Fe$_2$(CO)(PF$_2$=NMe)(μ-PF$_2$)(μ-MeN(PF$_2$)$_2$)$_3$, the P=N distance is 1.59(1) Å[31] so that, presuming this latter species has been correctly formulated, distinction between the MeNHPF$_2$ and [MeN=PF$_2$]$^-$ formulation cannot be made solely on the basis of the observed P—N distance. Unfortunately, no other data are available on the iron complex for a closer comparison but we believe that the data for **2** favor the proposed formulation. The coordination about ruthenium is of the typical "piano stool" type generally observed in cpRuL$_3$ complexes. The Ru—P(1) and Ru—P(2) distances to the PF$_2$NHMe ligands are essentially equivalent and are significantly shorter than that to the P(O)F$_2$ ligand (Ru—P(3) = 2.247(2) Å). This is consistent with the proposed formulation in that the π-acid character of the latter ligand should be diminished relative to that of the others because of the substantial π-bonding to oxygen. For comparison, the Ru—P distances to the less π-acidic ligand MeN(P(OMe)$_2$)$_2$ in cpRuCl(MeN(P(OMe)$_2$)$_2$) are 2.2384(5) and 2.244(5) Å.[8]

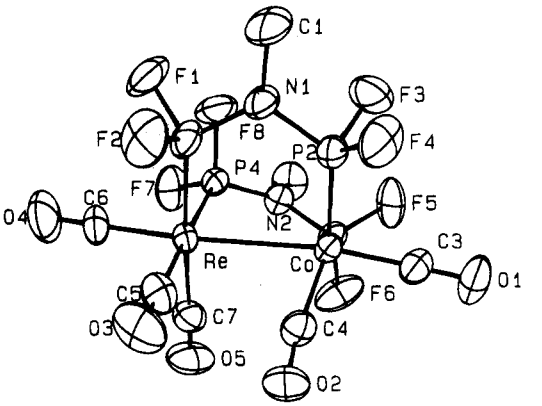

Figure 2. Perspective view of *fac*-Re(CO)$_3$(μ-MeN(PF$_2$)$_2$)$_2$-Co(CO)$_2$ (**5**). Thermal ellipsoids are drawn at the 50% probability level, and hydrogen atoms are omitted for clarity. P(1) is bonded to Re, F(1), and F(2). P(3) is bonded to Co, F(5), and F(6).

Table 7. Bond Distances (Å) and Interbond Angles (deg) for Re(CO)$_3$(μ-PNP)$_2$Co(CO)$_2$ (5)[a]

	Distances		
Re—Co	2.8932(9)	Co—C(3)	1.762(8)
Re—P(1)	2.328(2)	Co—C(4)	1.779(8)
Re—P(4)	2.324(2)	O(1)—C(3)	1.138(9)
Re—C(5)	1.996(9)	O(2)—C(4)	1.12(1)
Re—C(6)	1.915(8)	O(3)—C(5)	1.14(1)
Re—C(7)	1.992(9)	O(4)—C(6)	1.15(1)
Co—P(2)	2.083(2)	O(5)—C(7)	1.14(1)
Co—P(3)	2.076(2)		
	Angles		
Co—Re—P(1)	87.64(5)	Re—Co—P(2)	89.67(6)
Co—Re—P(4)	83.64(5)	Re—Co—P(3)	89.14(6)
Co—Re—C(5)	94.8(3)	Re—Co—C(3)	169.6(3)
Co—Re—C(6)	173.7(3)	Re—Co—C(4)	75.6(3)
Co—Re—C(7)	89.2(2)	P(2)—Co—P(3)	110.50(9)
P(1)—Re—P(4)	91.88(8)	P(2)—Co—C(3)	94.1(3)
P(1)—Re—C(5)	88.1(3)	P(2)—Co—C(4)	128.5(3)
P(1)—Re—C(6)	91.9(3)	P(3)—Co—C(3)	98.6(3)
P(1)—Re—C(7)	176.7(2)	P(3)—Co—C(4)	118.2(3)
P(4)—Re—C(5)	178.5(3)	C(3)—Co—C(4)	94.5(4)
P(4)—Re—C(6)	90.1(3)	Co—C(3)—O(1)	179.0(9)
P(4)—Re—C(7)	88.7(3)	Co—C(4)—O(2)	172.0(8)
C(5)—Re—C(6)	91.5(4)	Re—C(5)—O(3)	177.2(9)
C(5)—Re—C(7)	91.3(4)	Re—C(6)—O(4)	178.2(9)
C(6)—Re—C(7)	91.3(3)	Re—C(7)—O(5)	178.3(7)

[a] Numbers in parentheses are estimated standard deviations in the least significant digit.

(b) *fac*-Re(CO)$_3$(μ-MeN(PF$_2$)$_2$)$_2$Co(CO)$_2$ (5). A perspective view of **5** is presented in Figure 2, and pertinent bond distances and interbond angles in Table 7. There are no unusual intermolecular contacts in the solid. The Re—Co distance of 2.8932(9) Å is considerably longer than those found previously in (μ_3-*p*-tolyl)CReCo$_2$(CO)$_{10}$ (2.686(1), 2.720(1) Å)[32] and is also longer than the intraligand P- - -P contacts (P(1)- - -P(2) = 2.812(3), P(3)- - -P(4) = 2.798(3) Å), suggesting that metal—metal interaction is weak at best. As with other MeN(PF$_2$)$_2$-bridged heterobimetallic complexes reported previously[9,10] it is not clear whether to consider that **5** contains Re(0) and Co(0) or Re(I) and Co(−1) centers,

(28) Grosse, J.; Schmutzler, R.; Sheldrick, W. S. *Acta Crystallogr.* **1974**, *B30*, 1623.
(29) Dunitz, J. D.; Rollett, J. S. *Acta Crystallogr.* **1956**, *9*, 327.
(30) King, R. B.; Shimura, M.; Brown, G. M. *Inorg. Chem.* **1984**, *23*, 1398.
(31) Newton, M. G.; King, R. B.; Chang, M.; Gimeno, J. *J. Am. Chem. Soc.* **1978**, *100*, 326.
(32) Jeffrey, J. C.; Lewis, D. B.; Lewis, G. E.; Stone, F. G. A. *J. Chem. Soc., Dalton Trans.* **1985**, 2001.

but since the chemistry associated with the formation of **5** parallels that for cpFe(μ-MeN(PF_2)$_2$)$_2$Co(CO)$_2$,[10] we are inclined to favor the former formulation. With this assignment of oxidation state, at least a weak Re—Co interaction must exist to explain the diamagnetism of the complex. The two Re—CO distances *trans* to phosphorus are equivalent and their average, 1.994(2) Å, is significantly longer (Δ/σ = 8.7) than that to the axial carbonyl group (Re—C(6) = 1.915(8) Å), indicating a substantial structural *trans* influence of the phosphine ligands. The coordination about rhenium is distorted octahedral, with the major distortion being the displacement of the cobalt atom toward the vertex occupied by P(4), as indicated by the angles Co—Re—P(4) = 83.64(5)° and Co—Re—C(6) = 173.7(3)°, which may be the result of the "short-bite" of the PNP ligands and the weak Re—Co interaction. The coordination about cobalt is distorted trigonal bipyramidal and is quite similar to that found for the five-coordinate metal in Rh(CO)(μ-DPPM)$_2$M(CO)$_2$ (M = Co,[33] Rh,[34] Ir[35]; DPPM = bis(diphenylphosphino)methane). As with those, the distortion is seen in the angles between the equatorial ligands which vary from 110.50(9) to 128.5(3)° but more significantly in the angles Re—Co—C(3) = 169.6(3)° and Re—Co—C(4) = 75.6(3)°. This latter distortion is partly the result of the position of the cobalt relative to the rhenium, as noted above, but also is effectively due to a rotation of the {Co(CO)$_2$} unit about the Co—P(2) axis toward the rhenium. In the case of Rh(CO)(μ-DPPM)$_2$M(CO)$_2$ this last feature is occasioned by a semibridging interaction of the equatorial carbonyl with the rhodium, but here the Re—C(4) distance of 2.997(8) Å is too long for such an interaction. Also there are no unusually short intramolecular contacts between the carbonyl ligands and the phosphine ligands on cobalt, so there is no obvious reason for this distortion. The Re—P distances are equivalent and the average value, 2.326(2) Å, is significantly shorter than those found previously in [Rh(CH$_3$)(μ-CO)$_2$(μ-DPPM)$_2$Re(CO)$_2$](OTF)[36] and Re(N$_2$(*p*-tol))Cl(μ-CO)(μ-DPPM)$_2$PtCl[37] (*ca.* 2.43 Å), which is consistent with the greater π-acid character of the MeN(PF_2)$_2$ ligand. The Co—P distances are comparable to those found in cpFe(μ-MeN(PF_2)$_2$)$_2$Co(CO)$_2$,[10] and the remaining geometry of **5** is unexceptional.

(c) cpRu(μ-MeN(PF_2)$_2$)$_2$RhCl$_2$(PMe_2Ph) (9). A perspective view of **9** is shown in Figure 3, while pertinent bond distances and interbond angles appear in Table 8. There are no unusually short intermolecular contacts in the solid. The Rh—Ru distance of 2.8719(3) Å is long by comparison with most found previously, e.g. 2.697(1) Å in cpRu(μ-Ph_2PC(=CH_2)PPh_2)(μ-CO)$_2$RhCl$_2$,[38] 2.762(2) and 2.745(2) Å in [Ph_3)$_2$N][H_2Ru_3Rh(CO)$_{11}$(PPh_3)],[39] and 2.734(1) Å in H_2Ru_3Rh(μ-CO)(CO)$_6$(PPh_3)$_2$(μ-PPh_2)($PPhC_6H_4$).[40] In the last complex, the second Rh—Ru distance is 2.866(1) Å, which is close to that in

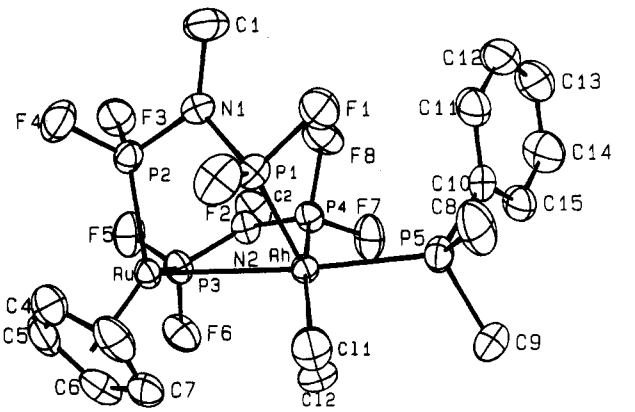

Figure 3. Perspective view of cpRu(μ-MeN(PF_2)$_2$)$_2$RhCl$_2$(PMe_2Ph) (**9**). Thermal ellipsoids are drawn at the 50% probability level, and hydrogen atoms are omitted for clarity.

Table 8. Bond Distances (Å) and Interbond Angles (deg) for cpRu(μ-PNP)$_2$RhCl$_2$ (PMe_2Ph) (9)[a]

	Distances		
Rh—Ru	2.8719(3)	Ru—P(3)	2.1726(9)
Rh—Cl(1)	2.3945(8)	Ru—C(3)	2.230(3)
Rh—Cl(2)	2.4496(9)	Ru—C(4)	2.220(4)
Rh-P(1)	2.1663(9)	Ru—C(5)	2.218(4)
Rh—P(4)	2.1559(8)	Ru—C(6)	2.249(4)
Rh—P(5)	2.3734(9)	Ru—C(7)	2.247(3)
Ru—P(2)	2.1552(9)		
	Angles		
Ru—Rh—Cl(1)	94.39(2)	Cl(2)—Rh—P(5)	95.13(3)
Ru—Rh—Cl1(2)	92.34(2)	P(1)—Rh—P(4)	95.87(3)
Ru—Rh—P(1)	69.04(2)	P(1)—Rh—P(5)	103.51(3)
Ru—Rh—P(4)	90.35(2)	P(4)—Rh—P(5)	93.72(3)
Ru—Rh—P(5)	171.88(3)	Rh—Ru—P(2)	97.64(2)
Cl(1)—Rh—Cl(2)	91.04(3)	Rh—Ru—P(3)	83.45(2)
Cl(1)—Rh—P(1)	91.24(3)	Rh—Ru—C′[b]	118.8(1)
Cl(1)—Rh—P(4)	172.51(3)	P(2)—Ru—P(3)	90.09(3)
Cl(1)—Rh—P(5)	82.31(3)	P(2)—Ru—C′[b]	128.7(1)
Cl(2)—Rh—P(1)	161.36(3)	P(3)—Ru—C′[b]	127.4(1)
Cl(2)—Rh—P(4)	82.97(3)		

[a] Numbers in parentheses are estimated standard deviations in the least significant digit. [b] C′ is the centroid of the cyclopentadienyl ring.

9 but it is accompanied by a Ph_2P bridge and so is not directly comparable. It is also slightly longer than the metal—metal distance found in the related complex cpFe(μ-MeN(PF_2)$_2$)$_2$IrCl$_2$(PMe_2Ph) (2.838(2) Å),[9] and as in the latter complex the metal—metal interaction that must exist in accord with the observed diamagnetism is relatively weak. This is further supported by the fact that the Ru—Rh distance is longer than the intraligand P- - -P separations (P(1)- - -P(2) = 2.642(1) Å, P(3)- - -P(4) = 2.794(1) Å). The overall geometry of **9** is quite similar to that found for the two independent molecules in the crystalline cpFe(μ-MeN(PF_2)$_2$)$_2$-IrCl$_2$(PMe_2Ph)[9] but with two notable differences. First, the rotational orientation of the dimethylphenylphosphine ligand places the phenyl group between the two —PF_2 groups bound to rhodium (see Figure S1, supplementary material) in contrast to eclipsing one or the other as occurs in the iron—iridium complex. As a consequence the hydrogen atom on C(11) makes a close contact (2.46 Å) with F(1) which twists that end of the MeN(PF_2)$_2$ ligand toward ruthenium. Second, while the Rh—Cl(1) distance is normal, that for Rh—Cl(2) is considerably longer and at the upper end of the range

(33) Elliot, D. J.; Ferguson, G.; Holah, D. G.; Hughes, A. N.; Jennings, M. C.; Magnuson, V. R.; Potter, D.; Puddephatt, R. J. *Organometallics* **1990**, *9*, 1336.
(34) Woodcock, C.; Eisenberg, R. *Inorg. Chem.* **1985**, *24*, 1287.
(35) McDonald, R.; Cowie, M. *Inorg. Chem.* **1990**, *29*, 1564.
(36) Antonelli, D. M.; Cowie, M. *Organometallics* **1990**, *9*, 1818.
(37) Carr, S. W.; Fontaine, X. L. R.; Shaw, B. L.; Thorton-Pett, M. *J. Chem. Soc., Dalton Trans.* **1988**, 769.
(38) Brown, M. P.; Burns, D.; Das, R.; Dolby, P. A.; Harding, M. M.; Jones, R. W.; Robinson, E. J.; Smith, A. K. *J. Chem. Soc., Dalton Trans.* **1991**, 351.
(39) Evans, J.; Stroud, P. D.; Webster, M. *J. Chem. Soc., Dalton Trans.* **1991**, 2027.
(40) Jungbluth, H.; Süss-Fink, G.; Pellinghelli, M. A.; Tiripicchio, A. *Organometallics* **1990**, *9*, 1670.

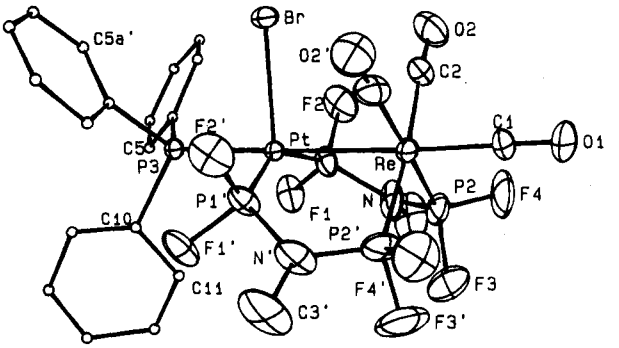

Figure 4. Perspective view of *fac*-$Re(CO)_3(\mu\text{-}MeN(PF_2)_2)_2PtBr(PPh_3)$ (**11**). Thermal ellipsoids are drawn at the 30% probability level. The primed atoms are related to their unprimed counterparts by the mirror. Only one orientation of the disordered triphenylphosphine and axial carbonyl ligands is shown, and hydrogen atoms are omitted for clarity.

Table 9. Bond Distances (Å) and Interbond Angles (deg) for $Re(CO)_3(\mu\text{-}PNP)_2PtBr(PPh_3)\cdot CH_2Cl_2$ (11)[a]

	Distances		
Pt—Re	2.8988(5)	Re—C(1)	1.91(2)
Pt—Br	2.738(1)	Re—C(2)	1.96(1)
Pt—P(1)	2.187(2)	C(1)—O(1)	1.16(2)
Pt—P(3)	2.354(2)	C(2)—O(2)	1.13(1)
Re—P(2)	2.306(3)		
	Angles		
Re—Pt—Br	89.36(3)	Pt—Re—C(2)	86.8(3)
Re—Pt—P(1)	83.69(6)	P(2)—Re—P(2)′	95.0(1)
Re—Pt—P(3)	178.64(6)	P(2)—R2—C(1)	87.2(4)
Br—Pt—P(1)	106.13(7)	P(2)—Re—C(2)	87.2(3)
Br—Pt—P(3)	89.28(7)	C(1)—Re—C(2)	86.7(5)
P(1)—Pt—P(1)′	145.08(3)	C(2)—Ru—C(2)′	90.3(4)
P(1)—Pt—P(3)	96.69(6)	Re—C(1)—O(1)	179(2)
Pt—Re—P(2)	88.82(7)	Re—C(2)—O(2)	176.5(9)
Pt—Re—C(1)	172.5(1)		

[a] Numbers in parentheses are estimated standard deviations in the least significant digit.

usually found for Rh—Cl bonds[41] but there is no obvious reason for this difference.

(d) *fac*-$Re(CO)_3(\mu\text{-}MeN(PF_2)_2)_2PtBr(PPh_3)\cdot CH_2Cl_2$ (11). A perspective view of **11** is shown in Figure 4, while pertinent bond distances and interbond angles appear in Table 9. There are no unusual intermolecular contacts in the solid. The core of the molecule has crystallographically imposed mirror symmetry, while the axial carbonyl ligand (C(4)O(1)) and the phenyl rings of the triphenylphosphine ligand are disordered across the mirror plane. The Re—Pt distance, 2.8988(5) Å, is somewhat longer than those for the unsupported Re—Pt bonds in $cpRe(H)(CO)_2Pt(H)(PPh_3)_2$ (2.838(1) Å)[42] and *trans*-$Pt(CO)_2(Re(CO)_5)_2$ (2.8309(5) Å)[43] and closer to that found in $Re(N_2(p\text{-}tol))Cl(\mu\text{-}DPPM)_2PtCl$ (2.859(4) Å).[37] Thus we conclude that significant Re—Pt bonding exists and, on the basis of the chemistry associated with its formation, formulate **11** as a Re(0)/Pt(I) species. The alternative formulation as a Re(−1)/Pt(II) species with a Re→Pt donor bond seems less likely as the values for $\nu_{C\equiv O}$ in **11** are only marginally lower than those in the Re(I) precursor (**3**). The Pt—P(1) distance, 2.187(2) Å, compares favorably with those found previously in $Pt_2(\mu\text{-}MeN(PF_2)_2)_3(PPh_3)$ (2.183(2)−2.252(2) Å) and $Mo(CO)_3(\mu\text{-}MeN(PF_2)_2)_2Pt(PPh_3)$ (2.206(4), 2.216(4) Å)[10] while the Re—P distances are slightly shorter than those found in **5**. The Pt—P(3) distance, 2.306(3) Å, also compares favorably with those to triphenylphosphine in $Pt_2(\mu\text{-}MeN(PF_2)_2)_3(PPh_3)$ (2.345(2) Å) and $Mo(CO)_3(\mu\text{-}MeN(PF_2)_2)_2Pt(PPh_3)$ (2.316(4) Å).[10] The most striking feature is the length of the Pt—Br bond (2.738(1) Å). This is substantially longer than typical terminal Pt—Br bonds which generally range from *ca.* 2.41 to 2.50 Å[41] and is significantly longer even than bridging Pt—Br bonds (*ca.* 2.63 Å).[41] It is however shorter than the apical Pt—Br bonds found in the distorted square pyramidal complexes $PtBr_2L_3$ (L = 5-Me,5-H-dibenzophosphole (3.026(3) Å), 5-Et,5-H-dibenzophosphole (3.143(3) Å)).[44] Considering the coordination geometry about the platinum we note that the P(1)—Pt—P(1)′ angle, 145.08(8)°, is about 10° smaller than the basal Br—Pt—P angles found in the above complexes but only slightly small than the corresponding P—Pd—Br angle in $PdBr_2$(5-ethyl-5-hydrodibenzophosphole)$_3$ (147.8(3)°).[44] In these phosphole complexes, the variation in the apical M—Br distance is thought to depend on electronic factors with a decrease in either the electron-donating power of the phosphole ligand or the basal Br—M—P angle strengthening, thereby decreasing the length of the M—Br bond. In **10**, therefore, we consider that the platinum has a distorted square pyramidal coordination with the strongly electron-withdrawing $MeN(PF_2)_2$ ligands tending to strengthen the apical Pt—Br bond as compared with what is seen in the phosphole complexes cited above. The coordination about rhenium is slightly distorted from ideal octahedral geometry, as evidenced by an opening of the P(2)—Re—P(2)′ angle to 95.0(1)° and a bending of the axial carbonyl ligand away from the metal—metal axis (Pt—Re—C(1) = 172.5(1)°). All other aspects of the structure appear unexceptional.

Conclusions

The results presented here not only demonstrate the utility of the "metalloligands" $cpRuCl(\eta^1\text{-}MeN(PF_2)_2)_2$ and *fac*-$ReBr(CO)_3(\eta^1\text{-}MeN(PF_2)_2)_2$ in the directed synthesis of heterobimetallic complexes but also indicate that halide transfer from these to the second metal is a continuing problem.

Acknowledgment. We thank the Chemistry Department of Tulane University for support of this work and Professor Max Roundhill for helpful discussions.

Supplementary Material Available: Complete tables of bond distances, interbond angles, calculated hydrogen atom positions, anisotropic thermal displacement parameters and rms amplitudes of anisotropic displacement for **2**, **5**, **9**, and **11** and figure showing an axial view of **9** (25 pages). Ordering information is given on any masthead page.

OM940218S

(41) Orpen, A. G.; Brammer, L.; Allen, F. H.; Kennard, O.; Watson, D. G.; Taylor, R. *J. Chem. Soc., Dalton Trans.* **1989**, S1.
(42) Casey, C. P.; Rutter, E. W., Jr.; Haller, K. J. *J. Am. Chem. Soc.* **1987**, *109*, 6886.
(43) Urbancic, M. A.; Wilson, S. R.; Shapley, J. R. *Inorg. Chem.* **1984**, *23*, 2954.
(44) Chui, K. M.; Powell, H. M. *J. Chem. Soc., Dalton Trans.* **1974**, 1879.